Bharat Bhushan, "Springer Handbook of Nanotechnology."

From these equations, one gets

$$F_z = \frac{12EI}{L^3}\left[z(L) - \frac{Lz'(L)}{2}\right],$$
$$F_x = \frac{2EI}{\ell L^2}\left[2Lz'(L) - 3z(L)\right]. \quad (11.33)$$

A second class of interesting properties of cantilevers is their resonance behavior. For cantilever beams one can calculate the resonant frequencies [11.147, 148]

$$\omega_n^{\text{free}} = \frac{\lambda_n^2}{2\sqrt{3}}\frac{h}{L^2}\sqrt{\frac{E}{\rho}} \quad (11.34)$$

with $\lambda_0 = (0.596864\ldots)\pi$, $\lambda_1 = (1.494175\ldots)\pi$, $\lambda_n \to (n+1/2)\pi$. The subscript n represents the order of the frequency, e.g., fundamental, second mode, and the nth mode.

A similar equation to (11.34) holds for cantilevers in rigid contact with the surface. Since there is an additional restriction on the movement of the cantilever, namely the location of its end point, the resonant frequency increases. Only the λ_n's terms change to [11.148]

$$\lambda'_0 = (1.2498763\ldots)\pi, \quad \lambda'_1 = (2.2499997\ldots)\pi,$$
$$\lambda'_n \to (n+1/4)\pi. \quad (11.35)$$

The ratio of the fundamental resonant frequency in contact to the fundamental resonant frequency not in contact is 4.3851.

For the torsional mode we can calculate the resonant frequencies as

$$\omega_0^{\text{tors}} = 2\pi\frac{h}{Lb}\sqrt{\frac{G}{\rho}}. \quad (11.36)$$

For cantilevers in rigid contact with the surface, we obtain the expression for the fundamental resonant frequency [11.148]

$$\omega_0^{\text{tors,contact}} = \frac{\omega_0^{\text{tors}}}{\sqrt{1+3(2L/b)^2}}. \quad (11.37)$$

The amplitude of the thermally induced vibration can be calculated from the resonant frequency using

$$\Delta z_{\text{therm}} = \sqrt{\frac{k_B T}{k}}, \quad (11.38)$$

where k_B is Boltzmann's constant and T is the absolute temperature. Since AFM cantilevers are resonant structures, sometimes with rather high Q, the thermal noise is not evenly distributed as (11.38) suggests. The spectral noise density below the peak of the response curve is [11.148]

$$z_0 = \sqrt{\frac{4k_B T}{k\omega_0 Q}} \quad (\text{in m}/\sqrt{\text{Hz}}), \quad (11.39)$$

where Q is the quality factor of the cantilever, described earlier.

11.3.2 Instrumentation and Analyses of Detection Systems for Cantilever Deflections

A summary of selected detection systems was provided in Fig. 11.8. Here we discuss in detail pros and cons of various systems.

Optical Interferometer Detection Systems

Soon after the first papers on the AFM [11.2] appeared, which used a tunneling sensor, an instrument based on an interferometer was published [11.149]. The sensitivity of the interferometer depends on the wavelength of the light employed in the apparatus. Figure 11.25 shows the principle of such an interferometeric design. The light incident from the left is focused by a lens on the cantilever. The reflected light is collimated by the same lens and interferes with the light reflected at the flat. To separate the reflected light from the incident light a $\lambda/4$ plate converts the linear polarized incident light into circular polarization. The reflected light is made linear polarized again by the $\lambda/4$-plate, but with a polarization orthogonal to that of the incident light. The polarizing

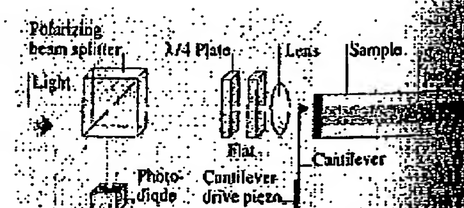

Fig. 11.25 Principle of an interferometric AFM. The light of the laser light source is polarized by the polarizing beam splitter and focused on the back of the cantilever. The light passes twice through a quarter wave plate and is orthogonally polarized to the incident light. The second arm of the interferometer is formed by the flat. The interference pattern is modulated by the oscillating cantilever